



저작자표시-비영리-동일조건변경허락 2.0 대한민국

이용자는 아래의 조건을 따르는 경우에 한하여 자유롭게

- 이 저작물을 복제, 배포, 전송, 전시, 공연 및 방송할 수 있습니다.
- 이차적 저작물을 작성할 수 있습니다.

다음과 같은 조건을 따라야 합니다:



저작자표시. 귀하는 원저작자를 표시하여야 합니다.



비영리. 귀하는 이 저작물을 영리 목적으로 이용할 수 없습니다.



동일조건변경허락. 귀하가 이 저작물을 개작, 변형 또는 가공했을 경우에는, 이 저작물과 동일한 이용허락조건하에서만 배포할 수 있습니다.

- 귀하는, 이 저작물의 재이용이나 배포의 경우, 이 저작물에 적용된 이용허락조건을 명확하게 나타내어야 합니다.
- 저작권자로부터 별도의 허가를 받으면 이러한 조건들은 적용되지 않습니다.

저작권법에 따른 이용자의 권리는 위의 내용에 의하여 영향을 받지 않습니다.

이것은 [이용허락규약\(Legal Code\)](#)을 이해하기 쉽게 요약한 것입니다.

[Disclaimer](#)

M.S. THESIS

NOVEL ENCODING METHOD USING
A PHOTOLUMINESCENT MATERIAL
FOR MICROPARTICLES
AND ITS APPLICATIONS

발광 물질을 이용한 새로운 마이크로입자 코드화
기법 및 응용

BY

TAEHONG KWON

FEBRUARY 2013

DEPARTMENT OF ELECTRICAL ENGINEERING AND
COMPUTER SCIENCE
COLLEGE OF ENGINEERING
SEOUL NATIONAL UNIVERSITY

NOVEL ENCODING METHOD USING A
PHOTOLUMINESCENT MATERIAL FOR
MICROPARTICLES AND ITS APPLICATIONS

발광 물질을 이용한 새로운 마이크로입자 코드화
기법 및 응용

지도교수 권 성 훈

이 논문을 공학석사 학위논문으로 제출함

2012년 11월

서울대학교 대학원

전기컴퓨터 공학부

권 태 홍

권태홍의 공학석사 학위논문을 인준함

2013년 2월

위원장 : 박 영 준

부위원장 : 권 성 훈

위원 : 김 성 재



Abstract

NOVEL ENCODING METHOD USING A PHOTOLUMINESCENT MATERIAL FOR MICROPARTICLES AND ITS APPLICATIONS

TAEHONG KWON

**DEPARTMENT OF ELECTRICAL ENGINEERING AND
COMPUTER SCIENCE**

**COLLEGE OF ENGINEERING
SEOUL NATIONAL UNIVERSITY**

Multiplexed assay technologies have been used in biological and medical studies on gene profiling, drug screening, and clinical diagnostics. An encoded suspension array was developed as a high-throughput, convenient, and low-cost method [1]. The encoded microparticles enabled easy handling of various molecules. A new encoding method needs to be developed to carry probe molecules in liquids and to identify them. This thesis presents a new encoding

method using the photoluminescent material 2,2-dimethoxy-2-phenylacetophenone (DMPA) and demonstrates its applications. First, perfluoropolyether microcapsules and disk-shaped microparticles were generated using hillock microfluidic channels and an optofluidic maskless lithography setup to test the feasibility of the encoding method [2]. Second, microparticle codes were created via diverse light patterns using the photoluminescence of DMPA. This new method has a high coding capacity and shows long-term durability. Furthermore, the code intensity can be controlled using DMPA concentration and ultraviolet light dose. As applications, the new multiplexed assay platform can be developed and code-changeable microparticles for multi-step assays can be fabricated.

Keywords: Multiplexed assay, Microparticles, Encoding, Photoluminescence, Microfluidics

Student Number: 2011-20794

Publications in Conference Proceedings

International Conference

- **T. Kwon**, Y. Song, D. Lee, M. Kim, T. Park, and S. Kwon, “Code-changeable Encoded Microparticles for Multi-step Bead-based Assay”, The 17th International Conference on Miniaturized Systems for Chemistry and Life Sciences (MicroTAS) 2012, Okinawa, Japan, October 2010. (Accepted for Poster Presentation)
- Y. Song, **T. Kwon**, D. Lee, J. Kim, D. Oh, and S. Kwon, “Encoding of Liquid Capped Microcapsule and Heterogeneous Assembly for Multiplexed Assay”, MicroTAS 2012, Okinawa, Japan, October 2010. (Accepted for Oral Presentation)
- Y. Song, **T. Kwon**, D. Lee, and S. Kwon, “Liquid Capped Encoded Microshell and Partipetting for Ultraplexed Liquid Assay”, Institute of Electrical and Electronics Engineers (IEEE) MEMS 2012, Paris, France, February 2012. (Poster)
- Y. Song, **T. Kwon**, D. Lee, and S. Kwon, “Liquid Capped Microshell and Partipetting for Multiplexed Assay”, Bubble Tech to Bio App “LAB-ON-A-CHIP”, Saarbrücken, Germany, October 2011. (Poster)

Domestic Conference

- **T. Kwon**, Y. Song, D. Lee, M. Kim, T. Park, and S. Kwon, “Graphically Writable Microparticle Generation Using a Photoluminescent Material for Bead-based Assay”, The Korean

Biochip Society 2012 Spring Conference, Ansan, Korea, May 2012.
(Poster)

- Y. Song, **T. Kwon**, D. Lee, and S. Kwon, “Generation of Microshell Particle for Liquid Encapsulation and Heterogeneous Assembly for Multiplexed Assay”, The 14th Korean Microelectromechanical Systems (MEMS) Conference, Jeju, Korea, April 2012. (Oral)

- Y. Song, **T. Kwon**, D. Lee, and S. Kwon, “Multiplexed Assay with Liquid Encapsulated Microshell and Partipetting”, The Korean Biochip Society 2011 Autumn Conference, Ulsan, Korea, November 2011. (Poster)

Contents

Abstract	ii
Contents	vi
List of Figures	viii
Chapter 1 Introduction	1
Chapter 2 Generation and Encoding of Microparticles Containing DMPA	3
2.1 Characteristics of DMPA Photoinitiator	4
2.2 Generation of Smart Microparticles Containing DMPA Photoinitiator	5
2.2.1 Sphere-shaped (core-shell) Microparticles Containing DMPA	5
2.2.2 Disk-shaped Microparticles Containing DMPA	17
2.2.3 Generation of Microparticle Codes	20
Chapter 3 Characterization of the Encoding Method Using DMPA Photoinitiator and its Applications	26
3.1 Characteristics of Microparticle Codes	26

3.1.1	Code Diversity	2 6
3.1.2	Code Durability	2 9
3.1.3	Code Intensity Controllability	3 2
3.1.4	Compatibility with Other Materials	3 5
3.2	Multiplexed Assay Platform Using Encoded Microcapsules	3 6
3.3	Code-changeable Microparticles for Multi-step Particle-based Assays	3 8
3.3.1	Repeated Code Writing	3 9
3.3.2	Silica-coating of Code-changeable Microparticles	4 0
Chapter 4	Conclusion	4 2
Supplementary Information		4 5
Possible Mechanisms of Code Photoluminescence		4 5
Bibliography		4 8
Abstract in Korean		5 4

List of Figures

Figure 2.1 Photoluminescence of the DMPA photoinitiator by UV light exposure: (A) Chemical structure of the DMPA; (B) DMPA photoinitiator becomes photoluminescent by UV irradiation; (C) Emission spectrum of DMPA photoinitiator after exposed to UV light (Excitation wavelength: 488 nm); (D) As the UV dose increased, the intensity of photoluminescence of DMPA also increased. The scale bar is 200 μm . [13].....	4
Figure 2.2 Schematic of PFPE core-shell microcapsule generation in the microfluidic channel with the hillock. [14].....	5
Figure 2.3 Computer-aided-design of the microfluidic channel with the hillock structure: (A) Layouts of the top and bottom layers; (B) Layout of the bottom layer; (C) The layout of the top layer; (D) Hillock design.....	7
Figure 2.4 Hydrophilicity test of the PDMS microfluidic channels: (A) The oil stream in the bare PDMS channel; (B) Oil droplets generated in the surface-modified PDMS microfluidic channels; (C) Oil droplets in the outlet; (D) Movement of the oil droplets into the outlet. The scale bar is 100 μm	10
Figure 2.5 Generation of PFPE droplets in the surface-modified PDMS microfluidic channel with the hillock structure. The scale bar is 200 μm	12

Figure 2.6 Generation of water-PFPE double emulsions in the surface-modified PDMS microfluidic channel with the hillock structure: (A) Fabrication of PFPE double emulsions in the hillock channel; (B) Gathered PFPE double emulsions at the outlet of the channel; (C) The PFPE double emulsions collected in a glass vial. The scale bar is 400 um.	1 3
Figure 2.7 Variations in the shape of water-PFPE double emulsions with the flow rate of the core water phase. The scale bar is 200 um. [14]	1 4
Figure 2.8 Variation in the diameters of whole and core droplets. [14]	1 4
Figure 2.9 Variations in the shape of water-PFPE double emulsions with the flow rate of the outer water phase. The scale bar is 200 um....	1 5
Figure 2.10 Solidified core-shell microparticles. The scale bar is 400 um. [14]	1 6
Figure 2.11 Schematic of microparticle generation using the Optofluidic Maskless Lithography System (OFML) and demonstration of sequential generation of diverse microparticles in the PDMS microfluidic channel. [2]	1 7
Figure 2.12 Disk-shaped PFPE microparticle generated by the OFML setup. The scale bar is 300 um.	1 8
Figure 2.13 Fabricated water-PFPE core-shell microcapsules and their encoding: (A) Produced water-PFPE core-shell microcapsules; (B) Encoded microcapsules. The scale bar is 250 um.	2 0
Figure 2.14 Verification of encoded regions of the microcapsules: (A) Confocal micrographs of the encoded microcapsules with different vertical positions; (B) Confocal micrograph of the triangular array-encoded microcapsule. (C) Confocal micrograph of the character A-encoded microcapsule. The scale bar is 100 um.	2 1
Figure 2.15 High-quantity encoding of disk-shaped microparticles: (A) Schematic of the high-quantity encoding of microparticles; (B) Triangular array pattern of the film mask (C) Fluorescent micrograph	

of the encoded microparticles using the setup in (A).	2 3
Figure 2.16 High-quantity encoding of core-shell microparticles. The scale bar is 250 μm	2 4
Figure 3.1 Code diversity of the encoded microcapsules: (A) Differently colored microcapsules and their codes. The insets represent the mask patterns. (B) The mixed microcapsules (C) The fluorescent images of encoded microcapsules. The scale bar is 250 μm	2 7
Figure 3.2 Code diversity of the encoded disk-shaped microparticles. Dotted lines represent particle boundaries. [13].....	2 9
Figure 3.3 Code durability with the different UV irradiation time for encoding microparticles. The scale bar is 250 μm	3 0
Figure 3.4 Code durability of the encoded microcapsules	3 0
Figure 3.5 Code durability of the disk-shaped encoded microparticles. [13]	3 1
Figure 3.6 Code intensity variation with the different concentrations of DMPA photoinitiator: (A) Relationship between DMPA concentration and code intensity; (B) Code intensity difference according to the variation of DMPA concentration. [13]	3 2
Figure 3.7 Code intensity variation with different UV irradiation times: (A) Relationship between UV irradiation time and code intensity; (B) The multi-level encoded microparticle. [13]	3 3
Figure 3.8 Magnetic particle-laden encoded microparticle generation: (A) Fabrication of magnetic-laden particle and its encoding; (B) Rotation of encoded microparticle by the magnetic force. [13].....	3 5
Figure 3.9 Multiplexed assay platform demonstration using encoded microcapsules. The scale bar is 200 μm	3 6
Figure 3.10 Schematic of the generation of code-changeable encoded microparticles using the OFML system. [13]	3 8
Figure 3.11 Code-changeability of encoded microparticles. The scale bar is 150 μm . [13].....	3 9
Figure 3.12 Silica-coated writable microparticle generation: (A) Bright-	

field micrograph of silica-coated microparticle; (B) Magnified view of the surface of silica-coated microparticle by scanning electron microscopy; (C) Fluorescent micrograph of the bare silica-coated microparticle; (D) Fluorescent micrograph of the encoded silica-coated microparticle. The scale bar is 200 μm . [13] 4 0

Figure S.1 Reactions of DMPA upon absorption of light [26] 4 5

Chapter 1

Introduction

Biological and medical studies on gene profiling, drug screening, and clinical diagnostics utilize multiplexed assays. Researchers obtain large amounts of information by allowing a sample to react with diverse probe molecules. In this context, high-throughput, convenient, and low-cost method for multiplexed assay need to be developed. Barcoded microparticles have attracted considerable attention from biological and medical researchers [1]. Microparticles with probe molecules that react with a sample are selectively observed with their barcodes, enabling researchers to easily determine the content of the sample. Improving the encoding method for microparticles enhances multiplexed assay platforms. In this context, this study introduces a new encoding method to improve existing multiplexed assay platforms.

Probe molecules can be mixed into a liquid vehicle. The liquid carrying the probe molecules can be encased in fabricated microcapsules. Several encoding methods can be utilized to distinguish between these microcapsules. Encoding materials such as quantum dots and DNA can be inserted into the core liquid region [3, 4]. However, because quantum dots are toxic, they can affect other liquid contents. In addition, DNA is not a good candidate for encoding microcapsules because nucleic acid sequences cannot be read in real-time. Another approach is to add fluorophores, such as fluorescent silica [5 - 8], quantum dots [3], and fluorescent organic dyes [9], to the microcapsule shells. By controlling the colors and intensity, the microcapsules can be encoded; however, their numbers are limited. The dynamic range of optical setups that detect fluorophores limits the number of combinations of fluorophores.

Two-dimensional graphical codes have high coding capacity. These codes include several lithographically fabricated microparticles [10-12]. Applying graphical coding to microcapsules can generate several codes unlike spectral coding. The succeeding chapters will introduce a new graphical encoding method for microparticles using a photoluminescent material, and discusses its characteristics and applications.

Chapter 2

Generation and Encoding of Microparticles Containing DMPA

In this chapter, the characteristics of a 2,2-dimethoxy-2-phenylacetophenone (DMPA) photoinitiator will be introduced. DMPA becomes photoluminescent when irradiated by UV light. This property can be utilized to encode microparticles. To demonstrate its feasibility, microparticles need to be fabricated, including core-shell microcapsules and disk-shaped microparticles. Core-shell microcapsules are created in hillock microfluidic channels, whereas disk-shaped microparticles are generated via an OFML setup. In addition, encoding microparticles using an OFML setup and high-quantity encoding method using film masks will be presented.

2.1 Characteristics of DMPA Photoinitiator

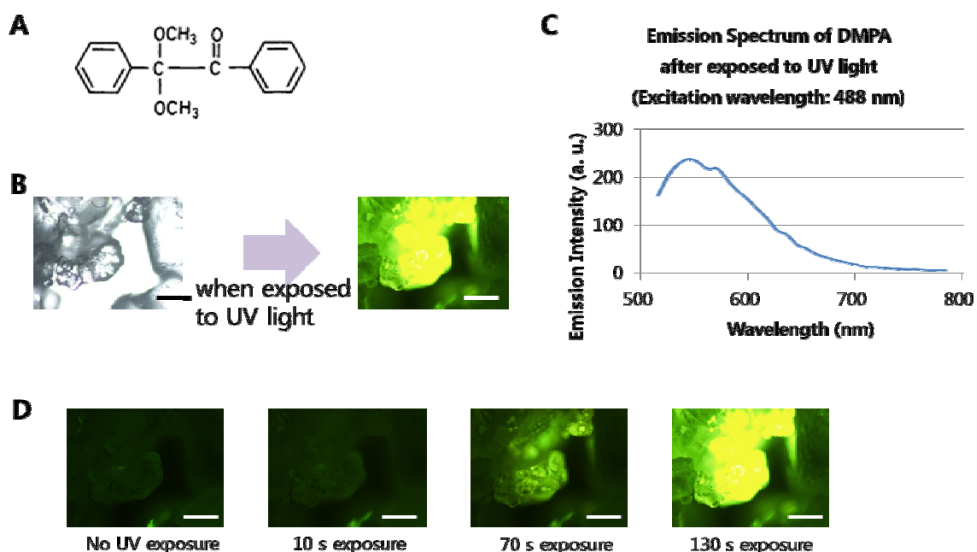


Figure 2.1 Photoluminescence of the DMPA photoinitiator by UV light exposure: (A) Chemical structure of the DMPA; (B) DMPA photoinitiator becomes photoluminescent by UV irradiation; (C) Emission spectrum of DMPA photoinitiator after exposed to UV light (Excitation wavelength: 488 nm); (D) As the UV dose increased, the intensity of photoluminescence of DMPA also increased. The scale bar is 200 μm . [13]

2,2-Dimethoxy-2-phenylacetophenone (DMPA) is a commonly used photoinitiator in photopolymerization. Figure 2.1 (A) shows the chemical structure of DMPA. It is mixed with acrylic and unsaturated polyester resins and it produces free radicals when irradiated with UV light. These radicals break the unsaturated bonds of resins and allow them to cross-link, which is the basic function of photocuring agents such

as DMPA. Aside from photopolymerization, DMPA is photoluminescent under UV irradiation. As shown in Figure 2.1 (B), the solid DMPA shows photoluminescence when the UV light is irradiated. The emission spectrum was obtained using a confocal microscope. It has a broad emission wavelength, and its peak wavelength is 544 nm. This photoluminescence intensity could be controlled with UV light. Figure 2.1 (D) shows that high doses of UV light increase the photoluminescence intensity.

2.2 Generation of Smart Microparticles Containing DMPA Photoinitiator

2.2.1 Sphere-shaped (core-shell) Microparticles Containing DMPA

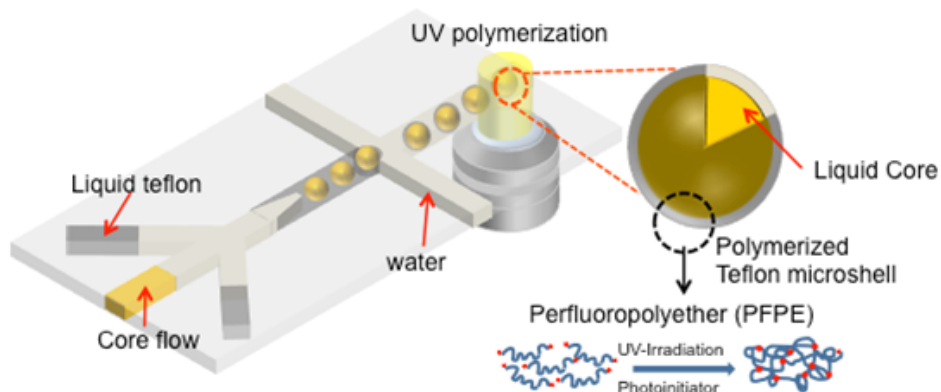


Figure 2.2 Schematic of PFPE core-shell microcapsule generation in the microfluidic channel with the hillock. [14]

To produce core-shell microparticles, I utilized the PDMS channel that had a hillock

structure. In 2010, Kim et al. introduced a microfluidic device that generates a three-dimensional coaxial flow by adding a simple hillock to produce alginate core-shell microcapsules to efficiently form cell spheroids [15]. Consequently, I used the microfluidic device to produce microcapsules with a hillock structure that could be easily made through photolithography in a fab.

The microfluidic channel with a hillock structure was made via a multi-level SU-8 fabrication method and a PDMS replica molding process. First, masks for the channel were drawn using AutoCAD software. One mask was for the hillock and the other mask was for the channel. The channel width was 200 μm , and the angle between the edges of the hillock was set to 60°. A mold for the microfluidic channel was produced using the two masks and an SU-8 negative photoresist. The SU-8 photoresist was poured onto the silicon wafer and spun. The spin speed was set to have a microstructure with a height of 25 μm . This structure was the first layer. After irradiating the mask for the channel with patterned light, the first layer with a height of 25 μm was produced. The second layer for the hillock was produced by pouring the photoresist onto the first layer and selectively photocuring it. Subsequently, the unphotopolymerized photoresist was removed using developing solution, and the microfluidic channel mold was finally produced.

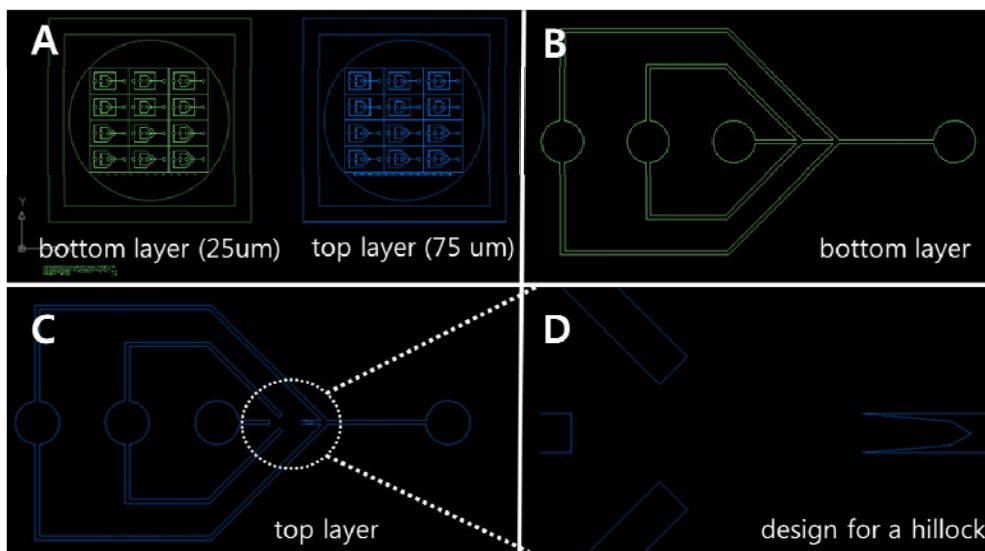


Figure 2.3 Computer-aided-design of the microfluidic channel with the hillock structure: (A) Layouts of the top and bottom layers; (B) Layout of the bottom layer; (C) The layout of the top layer; (D) Hillock design.

The PDMS channel with a hillock structure was produced using the SU-8 mold. The silicon wafer, which has an SU-8 channel mold, was attached to a glass dish by a transparent tape. Then PDMS (Sylgard 184; Dow Corning, Midland, MI) was mixed with the curing agent at a volume ratio of 10:1. This mixture was poured onto the SU-8 channel mold, and the solution was degassed in a vacuum chamber for 30 min. The solution was heated on a hotplate at 150 °C for 15 min. The PDMS slab was peeled off from the SU-8 mold and cut into several PDMS microfluidic channels. The complete PDMS microfluidic channel with a hillock structure requires the combination of two microfluidic channels. Therefore, two PDMS channels were

treated with oxygen plasma for 1 min, and then the channels were combined under a microscope.

To produce water-in-oil-in-water (W/O/W) double emulsions containing DMPA photoinitiator in the microfluidic channel, the outer path for the outer water phase needed to be hydrophilic. However, the PDMS channel was hydrophobic; therefore, a new method was needed to make the PDMS channel selectively hydrophilic. In 2010, Zagnoni demonstrated hysteresis in multiphase microfluidics at a T-junction [16]. He used the silane coupling agent 2-[methoxy(polyethyleneoxy)propyl]trimethoxysilane (SIM6492.7; Gelest, Tullytown, PA) to modify the PDMS surface to make it hydrophilic. When the PDMS surface was treated with oxygen plasma, hydroxyl functional groups ($-OH$) were created on the surface. The silane-coupling agent in solvent, such as toluene, also contains hydroxyl functional groups through hydrolysis and condensation. After the silane coupling agent in toluene was introduced into the oxygen plasma-treated PDMS microfluidic channel, the hydroxyl groups on the PDMS surface formed hydrogen bonds with the hydroxyl groups of the silane coupling agent. Finally, drying and curing allowed covalent bonds to form between the silane coupling agent and the PDMS substrate. In this manner, the hydrophilic monomer of the silane coupling agent was attached to the PDMS surface. The hydrophilicity of the modified PDMS channel was maintained for at least 7 days.

The PDMS channel surface was made hydrophilic as follows. First, the two slabs of the PDMS channel with a hillock were prepared. Holes for the inlets and outlets were created, and the slabs were washed with ethanol and dried with N₂. Then, the PDMS slabs were treated with oxygen plasma for 1 min. Before the hydroxyl groups of the PDMS surface disappeared, two slabs were attached to form one united channel with a height of 200 μm under a microscope. The bond between the two slabs was strong enough to allow the flow of liquids inside the channel. The bonded slabs were attached to a glass slide. Within 5 min, the silane coupling agent, 2-[methoxy(polyethyleneoxy)propyl]trimethoxysilane in toluene (at a volume ratio of 9:1) was introduced into the assembled channel using a suction equipment for 20 s. The solution residues and bubbles cause non-uniform surface modification. When the reaction solution was introduced into the channel with the suction equipment, the residues and bubbles were effectively removed. Moreover, the suction equipment allowed selective surface modification of the PDMS channel because the strong suction prevented liquid overflow from the outside to the hillock side. The channel was then left at room temperature for 5 min under pressure. The toluene was poured into the channel for several seconds, and the channel was washed with ethanol for 30 s. Channel integrity was maintained during the flowing process of these several liquids. Finally, the channel was heated on a hotplate at 100 °C for 10 min.

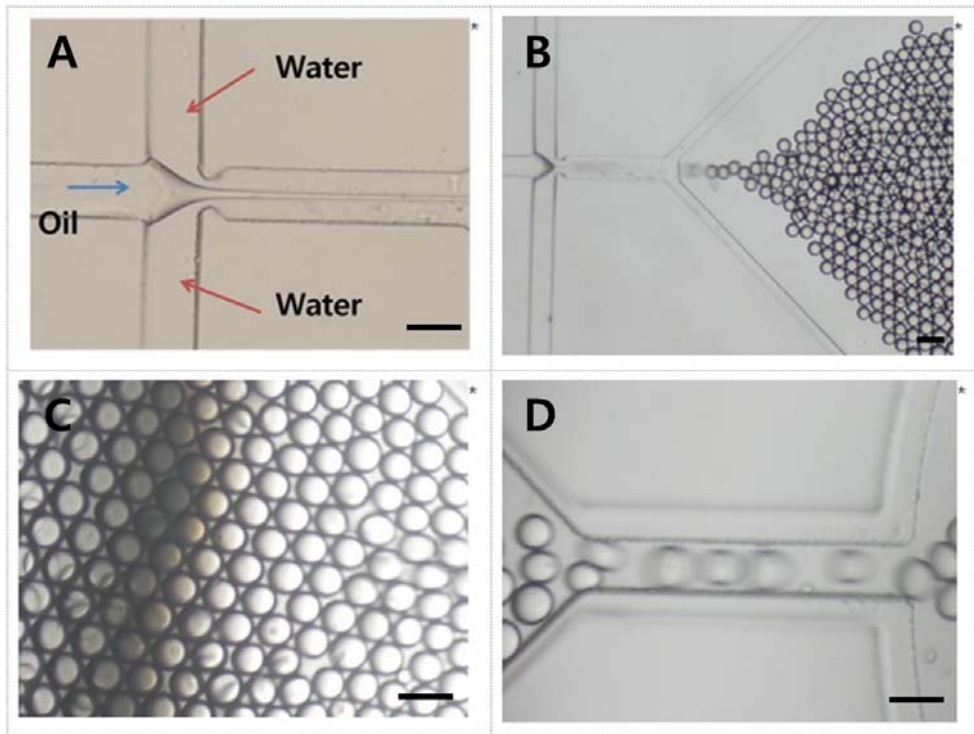


Figure 2.4 Hydrophilicity test of the PDMS microfluidic channels: (A) The oil stream in the bare PDMS channel; (B) Oil droplets generated in the surface-modified PDMS microfluidic channels; (C) Oil droplets in the outlet; (D) Movement of the oil droplets into the outlet. The scale bar is 100 μm .

To test the hydrophilicity of the microfluidic channel, the oil-in-water droplets in the microfluidic channel was generated. Oil-in-water droplets were produced in the hydrophilic PDMS channel. The untreated PDMS microfluidic channel was also prepared as a negative control. In this process, the PDMS channel without the hillock structure was used. The oil phase consisted of light mineral oil with span 80 surfactant at 5 wt.%, whereas the water phase contained deionized (DI)

water with Tween-20 surfactant at 5 wt.%. The flow velocities of the water phase and oil phase were 150 $\mu\text{L}/\text{h}$ and 10 $\mu\text{L}/\text{h}$, respectively. As shown in Figure 2.4 (A), oil-in-water droplets were not generated in the untreated PDMS microfluidic channel. The mineral oil phase was not cut into oil droplets by the water phase. The oil phase adhered onto the hydrophobic PDMS channel wall and continued to proceed into the outlet. By contrast, oil-in-water droplets were successfully produced in the surface-modified PDMS channel. At the same flow condition, the mineral oil phase was cut into the droplets and they could be collected at the outlet. In addition, the droplet size could be reduced by varying the flow rates of the water and oil phase. Based on this experiment, the surface of the PDMS can be effectively modified using 2-[methoxy (polyethyleneoxy)propyl]trimethoxysilane.

Methacrylic perfluoropolyether (PFPE; Fluorolink® MD 700, Solvay Solexis) was selected as the material for microcapsule shells. PFPE is an inert fluid that has low toxicity [17, 18]. Methacrylic PFPE shows water–oil repellence and high chemical resistance [19, 20]. Mixtures of methacrylic PFPE and photoinitiator can be photopolymerized under UV irradiation. Therefore, methacrylic PFPE can be used to encapsulate the various types of liquids. Given that PFPE is water repellent, PFPE can easily encapsulate water, but it does not dissolve in it.

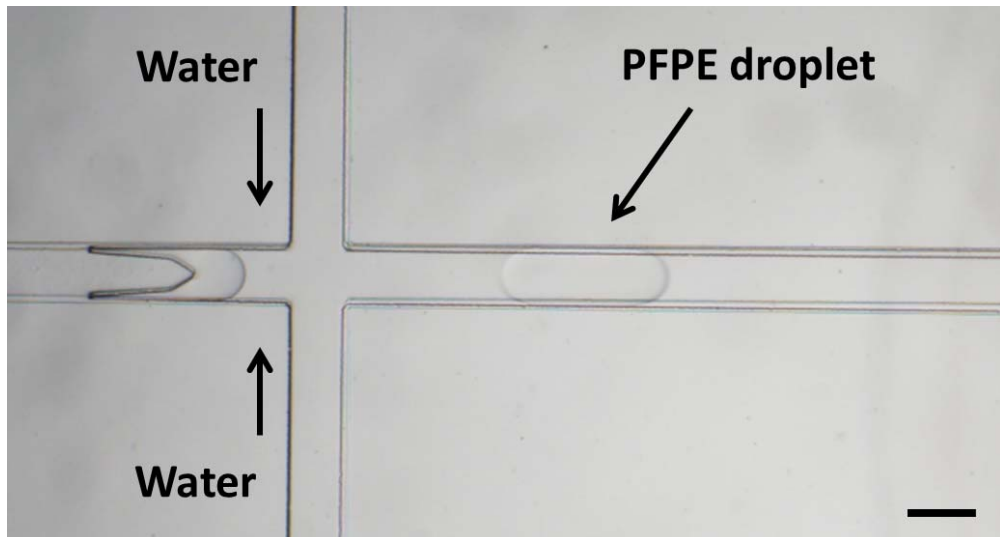


Figure 2.5 Generation of PFPE droplets in the surface-modified PDMS microfluidic channel with the hillock structure. The scale bar is 200 μm .

The production of PFPE single emulsions was initially demonstrated to generate water-in-PFPE-in-water double emulsions in the microfluidic channel with a hillock structure. The hillock microfluidic channel was prepared using the method described above. Then the PFPE was aspirated with a 1 mL syringe. To stabilize the droplets, 2 wt.% of surfactant was mixed with DI water. This solution was aspirated with a 30 mL syringe. Both syringes were installed in syringe pumps, and their contents were infused into the microfluidic channel through the tubes. The flow rates of PFPE and DI water were maintained at 200 $\mu\text{L/h}$ and 1000 $\mu\text{L/h}$, respectively. Considering the mineral oil droplets were produced in the hydrophilic PDMS channel, the PFPE droplets were successfully generated. Accordingly, I conclude

that the surface of the PDMS channel was modified to be hydrophilic, and this modified surface can be used to produce PFPE droplets.

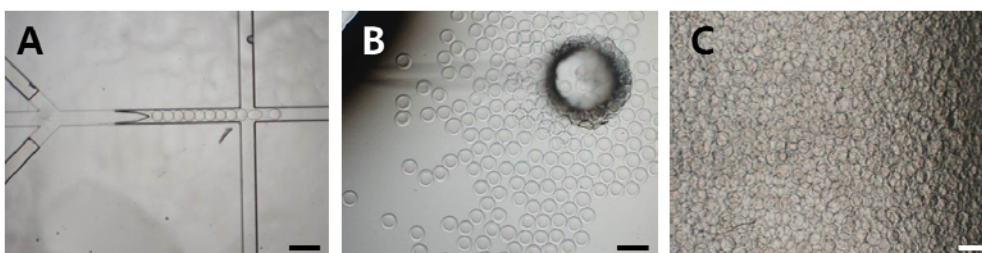


Figure 2.6 Generation of water-PFPE double emulsions in the surface-modified PDMS microfluidic channel with the hillock structure: (A) Fabrication of PFPE double emulsions in the hillock channel; (B) Gathered PFPE double emulsions at the outlet of the channel; (C) The PFPE double emulsions collected in a glass vial. The scale bar is 400 μm .

As a next step toward the generation of PFPE microcapsules, the DI water phase was introduced as the inner phase in the hillock microfluidic channel. It formed the coaxial flow as it passed the hillock structure. When the coaxial water phase met the slanted region of the hillock, the PFPE middle phase broke the water coaxial stream into water droplets. These droplets were aligned in the PFPE phase. At the cross junction, where the PFPE middle phase and DI water outer phase meet, the outer phase cut the water droplets-in-PFPE phase and generated water-in-PFPE-in-water double emulsions, as shown in Figure 2.6 (B). These double emulsions passed through the outlet of the channel and were collected in a vial. The water was

capsulated in the PFPE, and the PFPE shells had thickness of 20–30 μm .

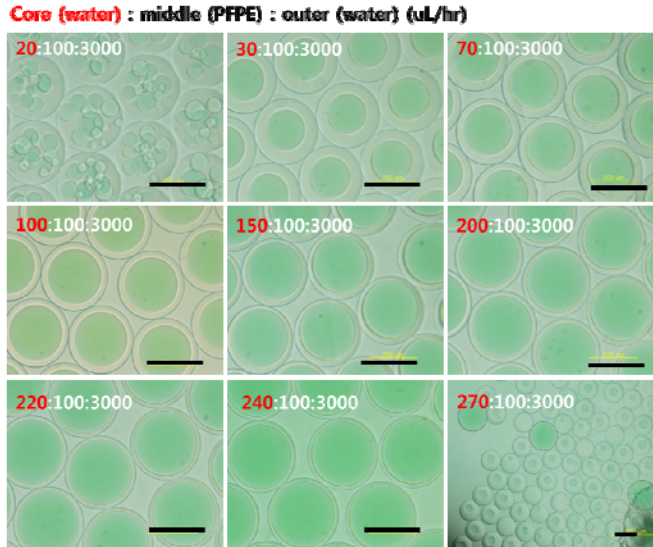


Figure 2.7 Variations in the shape of water-PFPE double emulsions with the flow rate of the core water phase. The scale bar is 200 μm . [14]

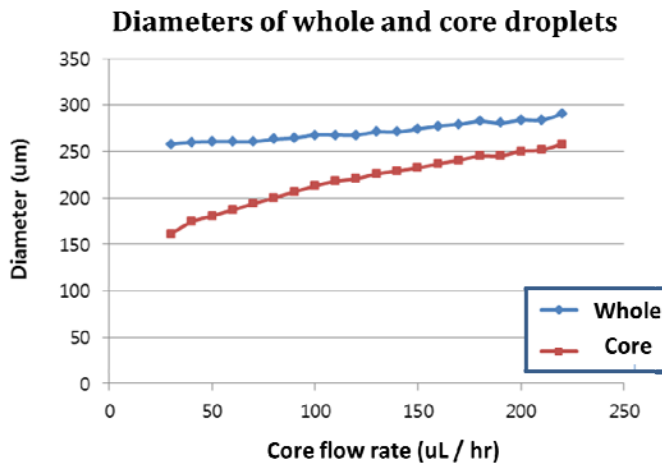


Figure 2.8 Variation in the diameters of whole and core droplets. [14]

Core (water) : middle (PFPE) : outer (water) ($\mu\text{L/hr}$)

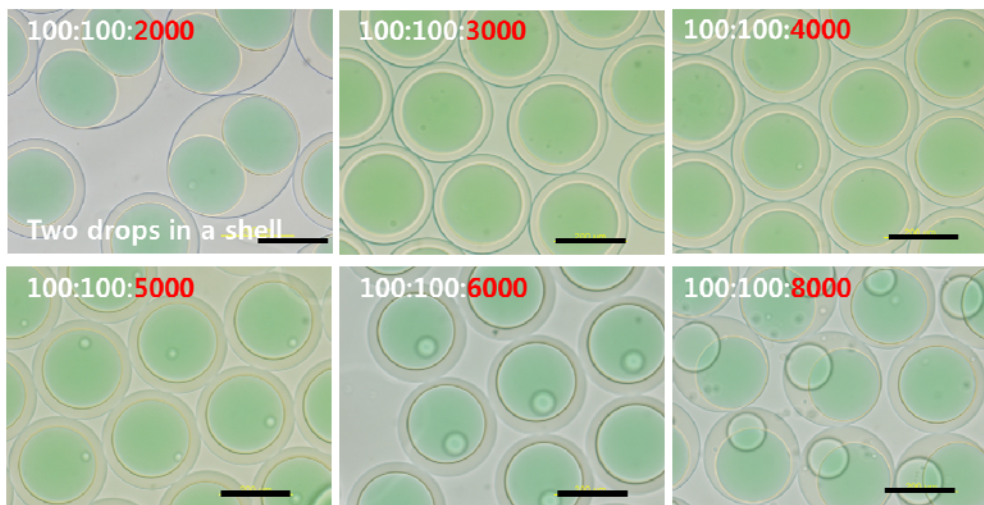


Figure 2.9 Variations in the shape of water-PFPE double emulsions with the flow rate of the outer water phase. The scale bar is 200 μm .

Diverse core liquid volumes and thickness were obtained by changing the flow rates of the core and the outer phases. The shell thickness and the core liquid volume depended on the flow rate of the core liquid water. To easily visualize these changes, a green food dye was used in this experiment. The flow rates of the middle and outer phases were set to 100 $\mu\text{L/h}$ and 3000 $\mu\text{L/h}$, respectively. As the flow rate increased, the overall size of the double emulsions remained almost the same. However, the volume of the core liquid increased, thereby decreasing the shell thickness. When the flow rate of the core phase was increased to 270 $\mu\text{L/h}$, the core liquid was no longer encapsulated in the PFPE shell. The generation of double

emulsions was unstable and produced various core volumes. By contrast, multiple core double emulsions were generated as the flow rate was decreased to 20 $\mu\text{L}/\text{h}$. The number of cores in the microcapsules can be controlled by limiting the flow rates.

Controlling the outer water phase did not significantly affect the overall size of the double emulsions. Multiple core double emulsions were produced at the flow rates of more than 4000 $\mu\text{L}/\text{h}$ and less than 3000 $\mu\text{L}/\text{h}$, when the flow rates of the core and middle phases were fixed to 100 $\mu\text{L}/\text{h}$.

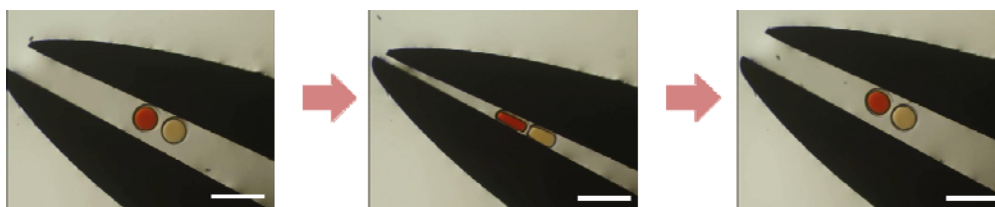


Figure 2.10 Solidified core-shell microparticles. The scale bar is 400 μm . [14]

To uniformly photopolymerize all double emulsions, the UV illumination setup was staged near the microscope. Double emulsions generated from the hillock microfluidic channel were moved to the outlet. The tube was inserted into the outlet to allow the double emulsions to flow into the tube. This tube was positioned in the UV illumination box so that the emulsions were polymerized while moving in the tube. These microparticles were collected in a glass vial. In this manner, photopolymerized microcapsules were generated.

2.2.2 Disk-shaped Microparticles Containing DMPA

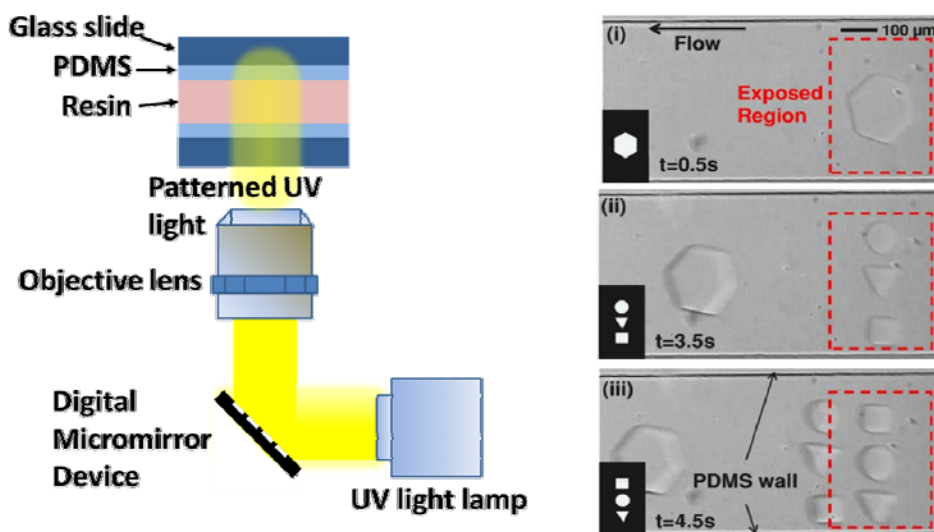


Figure 2.11 Schematic of microparticle generation using the Optofluidic Maskless Lithography System (OFML) and demonstration of sequential generation of diverse microparticles in the PDMS microfluidic channel. [2]

Chung et al. developed the OFML setup in 2007 [2]. In this research, free-floating polymeric microstructures were dynamically synthesized inside the microfluidic channels. The OFML setup allowed photocurable resin to be selectively polymerized with high-speed two-dimensional spatial light modulators. The timing and location of the photopolymerization process could be precisely controlled. Therefore, microparticles with various sizes and shapes could be easily fabricated in the

microfluidic channel.

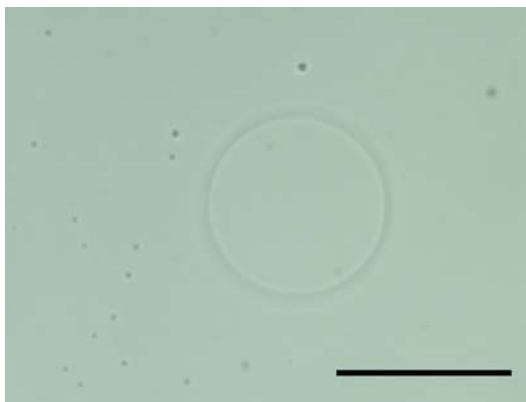


Figure 2.12 Disk-shaped PFPE microparticle generated by the OFML setup. The scale bar is 300 μm .

Using the OFML setup, disk-shaped microparticles containing DMPA photoinitiator could be fabricated. DMPA photoinitiator (5 wt%) was mixed with methacrylic PFPE. This solution was rigorously vortexed for 30 min. Then, this solution was dropped on the glass slide. The spacers (150 μm thick) were placed at the ends of the glass slide. The thickness of disk-shaped microparticles was controlled using the thickness of spacers. Then, another glass slide was placed on the solution. The space between the two glass slides was filled with the solution of methacrylic PFPE and DMPA photoinitiator. The assembled parts were placed on the microscope. To fabricate disk-shaped circular microparticles, the circle image was uploaded to the software, which controlled a digital micromirror device. After the UV light from a light source reached the micromirror device, a circular pattern of

light was produced. This patterned light was focused on the photopolymerizable resin through the objective lens. The UV light illumination time was set to 1 s. The disk-shaped circular microparticles were created via photopolymerization, as described in the figure above. The particles remained attached to the glass slide. The uncured monomer was removed by DI-water and a nitrogen gun. The remaining PFPE microparticles were detached from the glass slide with a razor and collected in a glass vial.

The number of generated PFPE microparticles was increased using a motorized stage. To fabricate numerous microparticles, the UV illumination area needed to be changed continuously so that different particles were generated in the different areas. Manually moving the stage was time consuming and labor intensive. To overcome these limitations, the motorized stage was used to make disk-shaped PFPE microparticles. Using the lab-made software, the stage moved horizontally and vertically with the predetermined distance. Whenever the stage moved, the patterned UV light directed at the methacrylic PFPE solution, resulting in the photopolymerization of the solution. Thus, the microparticle array was fabricated automatically.

2.2.3 Generation of Microparticle Codes

As described earlier, the DMPA photoinitiator is photoluminescent under UV irradiation. The DMPA photoinitiator has two functions: to produce free radicals for polymerization of methacrylic PFPE and to generate photoluminescence. The OFML setup is able to create diverse patterns of UV light. The additional UV light pattern could be used to generate microparticle codes.

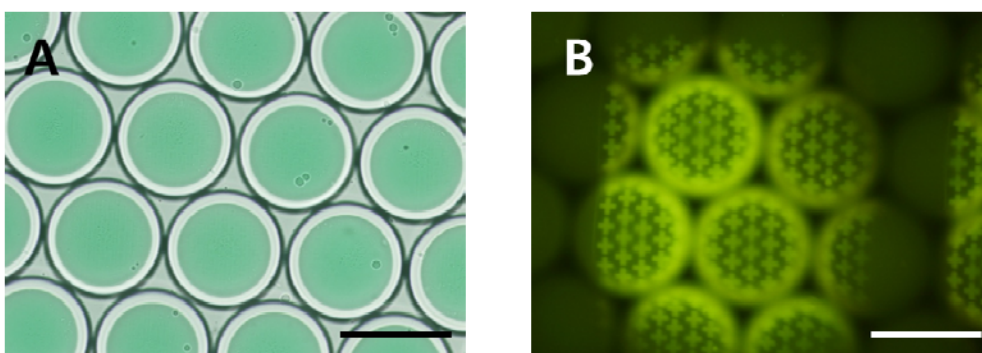


Figure 2.13 Fabricated water-PFPE core-shell microcapsules and their encoding: (A) Produced water-PFPE core-shell microcapsules; (B) Encoded microcapsules. The scale bar is 250 μm .

The microcapsules with water-based liquids in the core were successfully produced in the hillock microfluidic channel. These capsules already had PFPE shells. The PFPE shells contained the DMPA photoinitiator. Diverse patterns such as circles, squares, triangles, and hearts could be loaded into the software, and the OFML setup could be used to create UV light patterns. The light patterns were

focused onto the PFPE shells of microcapsules through the objective lens. The focal plane was centered at the bottom half of the capsules. As in the figure above, the unique codes of microcapsules were generated using the patterned UV light. The codes were not observable in the bright field. The fluorescent codes of the shells were clearly observed using a fluorescence illumination source and a filter. The microcapsules had cross arrays on shells. This result demonstrates that the microcapsules could be distinguished by observing the fluorescent codes.

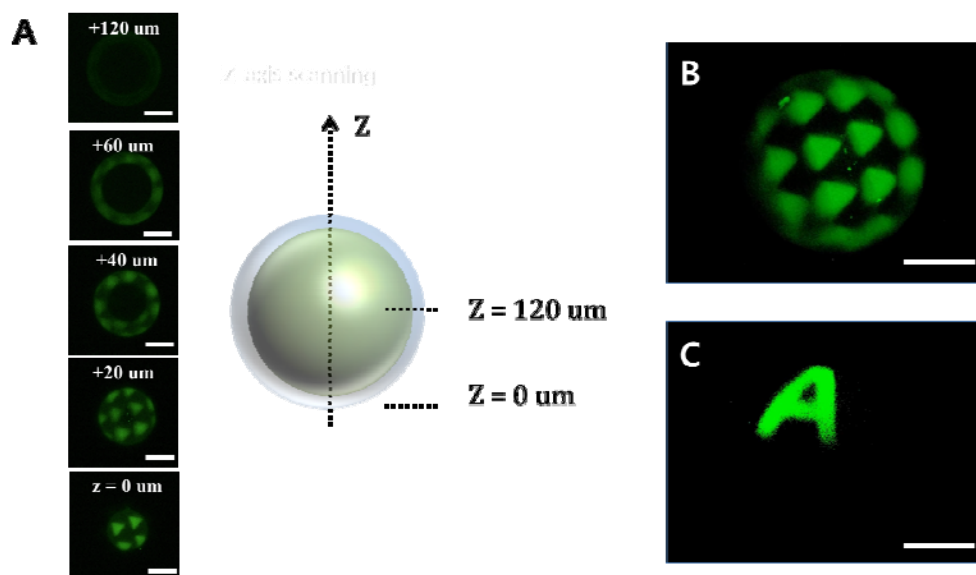


Figure 2.14 Verification of encoded regions of the microcapsules: (A) Confocal micrographs of the encoded microcapsules with different vertical positions; (B) Confocal micrograph of the triangular array-encoded microcapsule. (C) Confocal micrograph of the character A-encoded microcapsule. The scale bar is 100 um.

Confocal images of microcapsules were captured to verify the presence of fluorescent codes on the microcapsule shells. The microcapsules were 240 μm in diameter. The microcapsules were scanned vertically from the bottom ($z = 0 \mu\text{m}$) to the center ($z = 120 \mu\text{m}$). Only PFPE shells were observed at the bottom of the capsules so that triangular fluorescent codes were observed without hollow circles. As the scan plane progressed up to $z = 20 \mu\text{m}$, more codes were observed because the shell regions expanded. At $z = 40 \mu\text{m}$, the hollow black circular region was observed inside the fluorescent code region, which indicates that the fluorescent codes were only present in microcapsule shells, not in the liquid in the core. As the scan plane moved further, the codes were confirmed to be present only in the shells. The figures on the right describe the three-dimensional fluorescent images of the microcapsules. The triangular code array was in the shells. Code thickness equaled the shell thickness of the capsules. Moreover, the character “A” in the shells seemed to bend due to the spherical shape of the core-shell microparticles.

In addition to the microcapsules, the fluorescent codes were generated on the disk-shaped microparticles. The produced microparticles were placed on the slide glass and exposed to patterned UV light. The time to encode microparticles in the field of view of the microscope was 20 s. The fluorescent codes of microparticles were observed through fluorescence microscopy. The code pattern showed brighter fluorescence, whereas the uncoded region had no fluorescence.

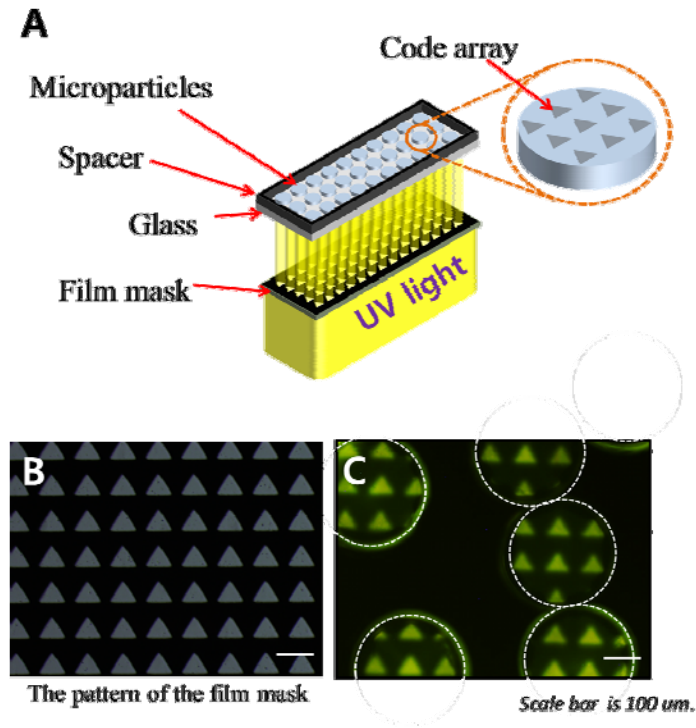
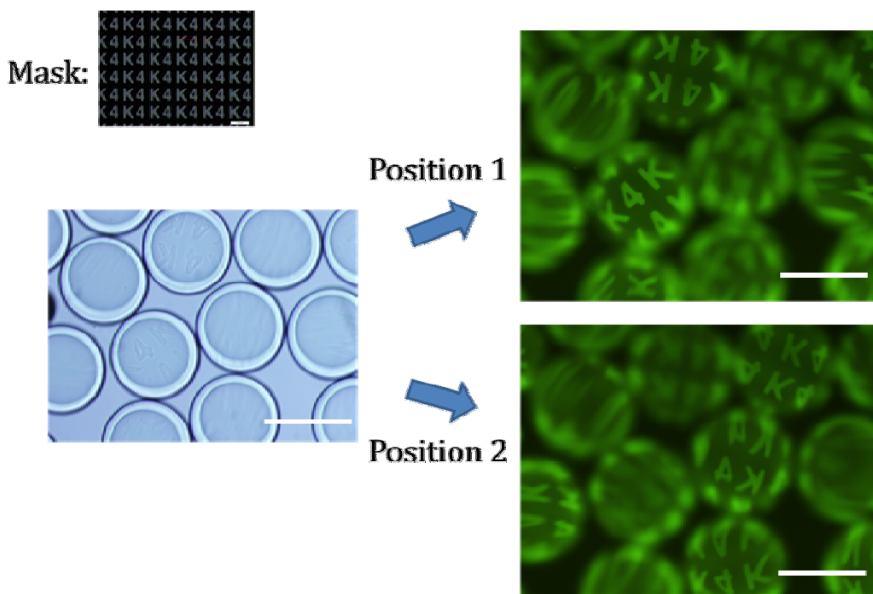


Figure 2.15 High-quantity encoding of disk-shaped microparticles: (A) Schematic of the high-quantity encoding of microparticles; (B) Triangular array pattern of the film mask (C) Fluorescent micrograph of the encoded microparticles using the setup in (A).



Images at the different focus positions

Figure 2.16 High-quantity encoding of core-shell microparticles. The scale bar is 250 μm .

Encoding the core-shell and disk-shaped microparticles in the field of view of the microscope required about 20 s. Considering the microscopic field contained 10 microparticles, this encoding method was not appropriate for the high-quantity encoding of core-shell and disk-shaped microparticles. For example, for 10,000 microparticles, $10,000/(10 * 20) = 20,000 \text{ s} = \text{about } 333 \text{ m} = \text{about } 5 \text{ h and } 30 \text{ minutes}$ were needed, which is time consuming. A new encoding method was developed to achieve high-quantity encoding of disk-shaped and core-shell microparticles. As shown in Figure 2.15 (A), the film-combined-glass mask (FCG mask; Microtech) was used to generate patterned UV light. The FCG mask consisted

of the glass (2 mm in height) and the film. Diverse pattern arrays were represented in the mask using commercial CAD software. Figure 2.15 (B) shows the mask pattern of the triangle array. The patterned film was attached to the glass. The resolution of the mask was 20 μm , which was sufficient to generate microparticle codes. The microparticles were placed on the FCG mask to mark the particles. Then, UV light from the illumination source was irradiated from the bottom of the mask. When the UV light passed through the mask, the opaque parts of the mask blocked the UV light. Thus, the only patterned UV light reached the microparticles, which created the fluorescent codes. Considering the illuminated region is not limited to the field of view of the microscope and whole microparticles on the mask could be exposed to UV, high-quantity encoding of microparticles was feasible. As described in Figure 2.15 (C), the microparticles were successfully encoded using the new encoding method. Aside from disk-shaped microparticles, high-quantity encoding was successfully demonstrated for core-shell microcapsules. Figure 2.16 shows that the character “K4” was encoded on the core-shell microparticles. Different focus positions were used to identify each code because particle positions were not on the same vertical planes before UV irradiation and particles were moved for imaging.

Chapter 3

Characterization of the Encoding Method Using DMPA Photoinitiator and its Applications

The PFPE core-shell microcapsules and disk-shaped microparticles containing DMPA photoinitiator were produced, as described in Chapter 2. These particles were encoded by the diverse patterns of UV light. In this chapter, several properties of the encoding method using DMPA photoinitiator are introduced and its applications are demonstrated.

3.1 Characteristics of Microparticle Codes

3.1.1 Code Diversity

To distinguish between different microcapsules or disk-shaped particles, each microparticle needs to have a unique code. Therefore, a new encoding method for microparticles should have high coding capacity. The new encoding method using photoluminescent DMPA photoinitiator produces diverse codes for microparticles because numerous light patterns can be created using the OFML system. Any

graphical code can be drawn in the software and then its image file can be transformed into a unique light pattern through the digital micromirror device and controller software.

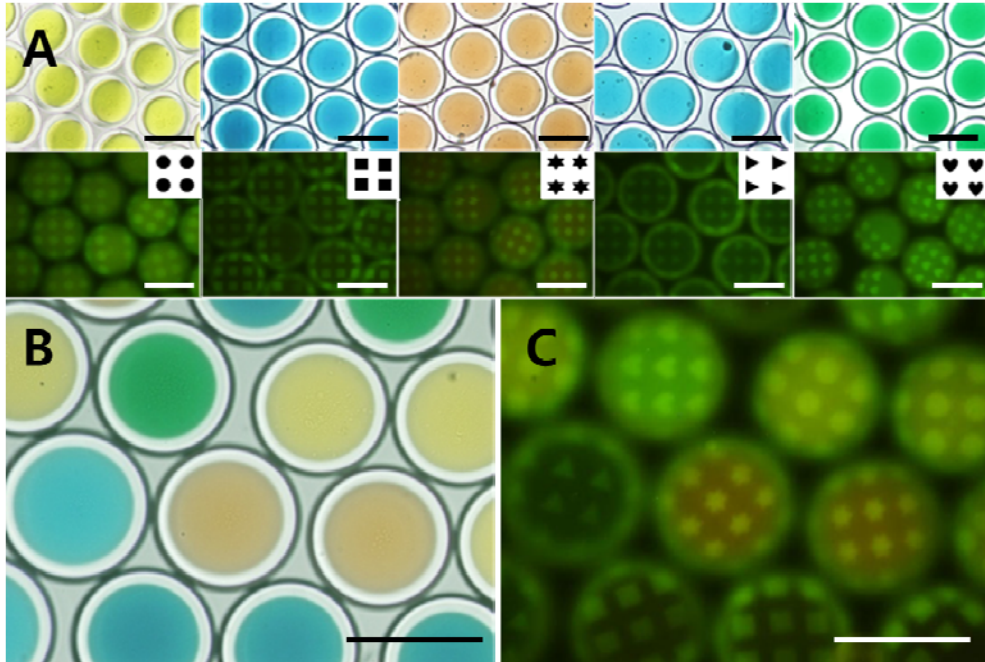
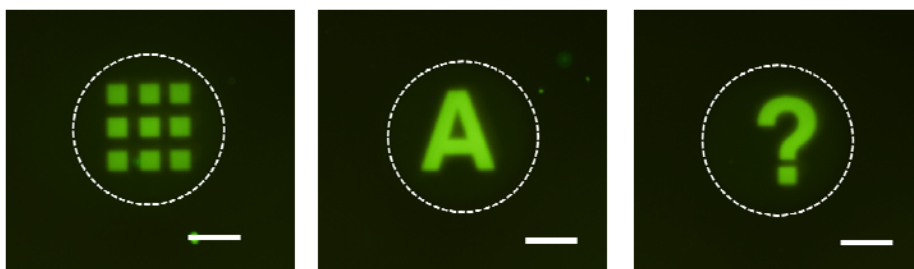


Figure 3.1 Code diversity of the encoded microcapsules: (A) Differently colored microcapsules and their codes. The insets represent the mask patterns. (B) The mixed microcapsules (C) The fluorescent images of encoded microcapsules. The scale bar is 250 μm .

The microcapsules were used first to show the code diversity of the new encoding method. The microcapsules with water-based liquids in the core were successfully produced in the hillock microfluidic channel, as previously described.

These capsules already had PFPE shells. The PFPE shells contained DMPA photoinitiator. The diverse patterns such as circles, squares, triangles, and hearts were loaded into the software. The UV light patterns were created using the OFML setup. The mask image files are shown in the insets of the top figures. The light patterns were focused onto the PFPE shells of microcapsules through the objective lens. The focal plane was centered on the bottom half of the capsules. As shown in the figure above, four different microcapsules were produced. These capsules had unique colors since different food dyes were used for each microcapsule. The unique codes of microcapsules were generated using the patterned UV light. The codes were not observable under bright field microscopy. The fluorescent codes on the shells were clearly observed using a fluorescence illumination source and a filter. For example, the yellow microcapsules had circle array on the shells. The blue and green microcapsules showed fluorescent triangle and heart arrays, respectively. The bottom figures demonstrate that the microcapsules could be distinguished by observing the fluorescent codes. All types of colored microcapsules were collected in a vial and each fluorescent code was matched with each color. Other unique codes could also be generated aside from the graphical codes in the figures.



Scale bar is 100 μ m.

Figure 3.2 Code diversity of the encoded disk-shaped microparticles. Dotted lines represent particle boundaries. [13]

The disk-shaped microparticles containing DMPA can also have diverse graphical codes as the core-shell microcapsule can. The top figures show the fluorescent images of the encoded disk-shaped microparticles. Diverse graphical patterns such as square array, character A, and question mark can be encoded on the particles. Since these codes were not erasable, the other additional codes could be produced in the uncoded regions.

3.1.2 Code Durability

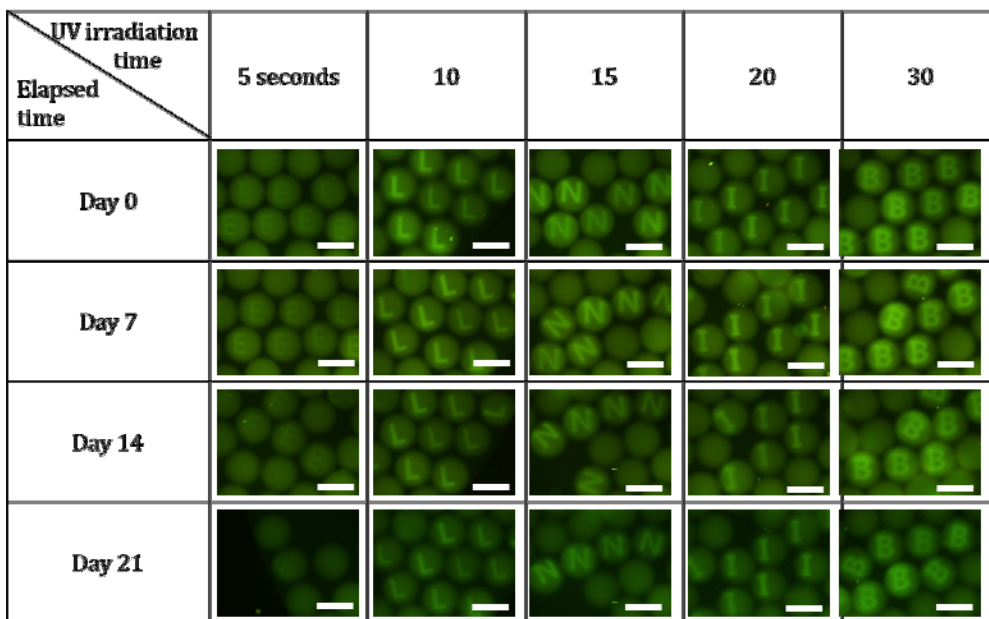


Figure 3.3 Code durability with the different UV irradiation time for encoding microcapsules. The scale bar is 250 μm .

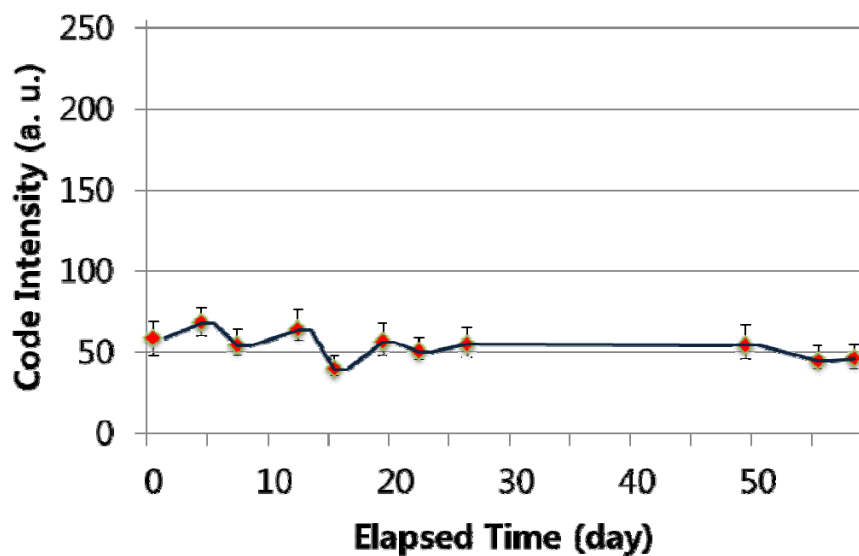


Figure 3.4 Code durability of the encoded microcapsules

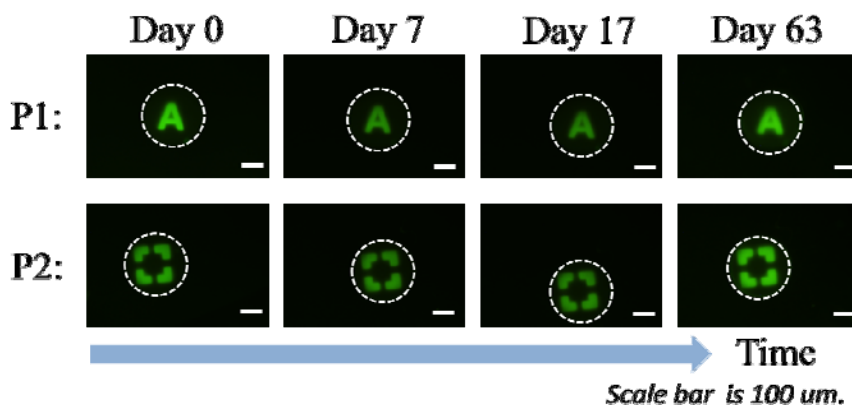


Figure 3.5 Code durability of the disk-shaped encoded microparticles. [13]

The microparticle codes should persist for a long time. If the codes disappear as soon as they are generated, the different microparticles with different biochemical contents cannot be distinguished from each other. Therefore, the codes need to maintain their intensity for a long time. Microcapsules were prepared and encoded to test the durability of code. These microparticles were stored in DI-water. Different characters on the shells indicate different UV irradiation times (character E: 5 s, L: 10 s, N: 15 s, I: 20 s, B: 30 s). Except for the E, all other cases exhibited code durability. Specifically, the fluorescent codes maintained their intensity to help users easily recognize their codes. No significant decrease in code intensity was observed in these cases. Thus, UV illumination needs at least 10 s at 180 mW/cm^2 to generate codes. Among the encoded microcapsules, code character B was continuously

monitored for about 2 months. As illustrated in the center figure, the code intensity remained almost the same for 2 months. In addition to the capsules, the disk-shaped particles showed long-term code durability, as described in the bottom figure. In summary, generated codes have long durability.

3.1.3 Code Intensity Controllability

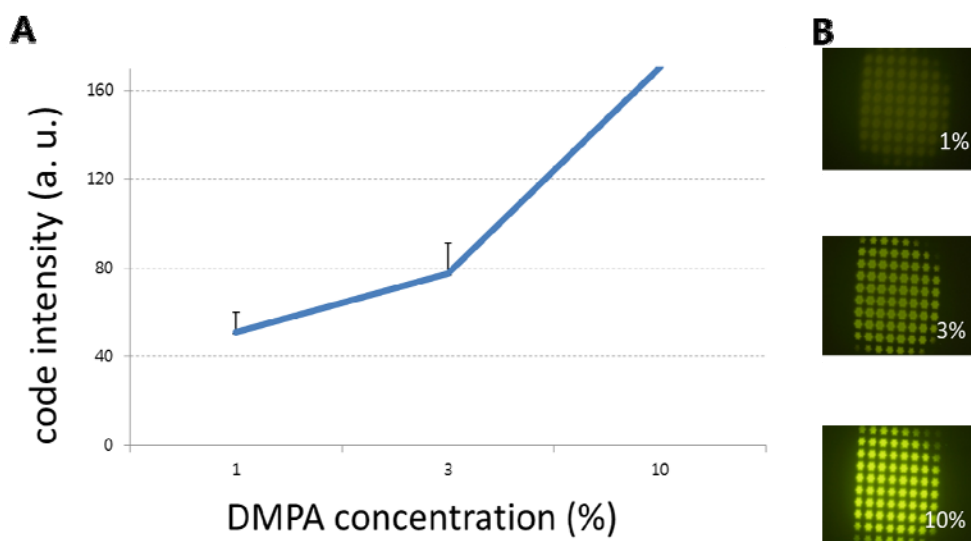
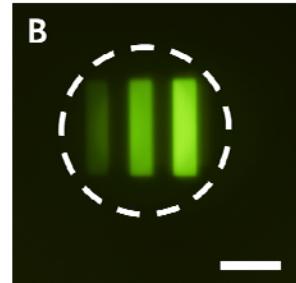
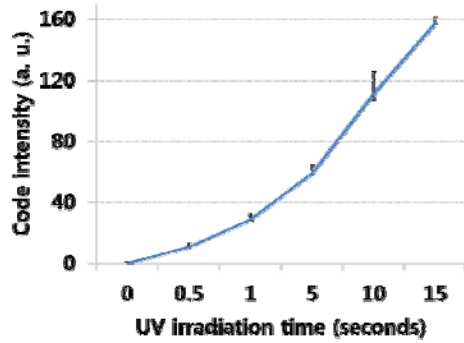


Figure 3.6 Code intensity variation with the different concentrations of DMPA photoinitiator: (A) Relationship between DMPA concentration and code intensity; (B) Code intensity difference according to the variation of DMPA concentration. [13]

A

Scale bar is 100 μm .

Figure 3.7 Code intensity variation with different UV irradiation times: (A) Relationship between UV irradiation time and code intensity; (B) The multi-level encoded microparticle. [13]

The code intensity could be varied. Figure 3.6 and 3.7 indicates that code intensity depends on the initiator concentration in the PFPE resin and on the UV irradiation time. The PFPE solutions with three different concentrations of DMPA photoinitiator, namely, 1 wt%, 3 wt%, and 10 wt%, were prepared. These solutions were poured onto glass slides and exposed to the patterned UV light at 180 mW/cm^2 . The fluorescent images were captured and the pixel color information was sampled. The intensity values were calculated and plotted on the graph, as illustrated in Figure 3.6 (A). Given that the DMPA photoinitiator itself is photoluminescent under UV light, the intensity increased as the amount of photoinitiator increased. UV irradiation time affects the code intensity. The power of patterned UV light was fixed at 180 mW/cm^2 . The UV illumination time varied from 0 s to 120 s. After the codes were

generated according to each illumination time, the intensity was calculated and plotted on the graph, as described in Figure 3.7 (A). The intensity of the codes increased with illumination time. Thus, a higher concentration of DMPA photoinitiator and longer UV irradiation time increased the photoluminescence intensity of the codes. Therefore, the photoluminescence of the codes could be adjusted using these two parameters. Figure 3.7 (B) shows an example of three-level codes in the microparticle. These codes were produced by varying UV irradiation time.

3.1.4 Compatibility with Other Materials

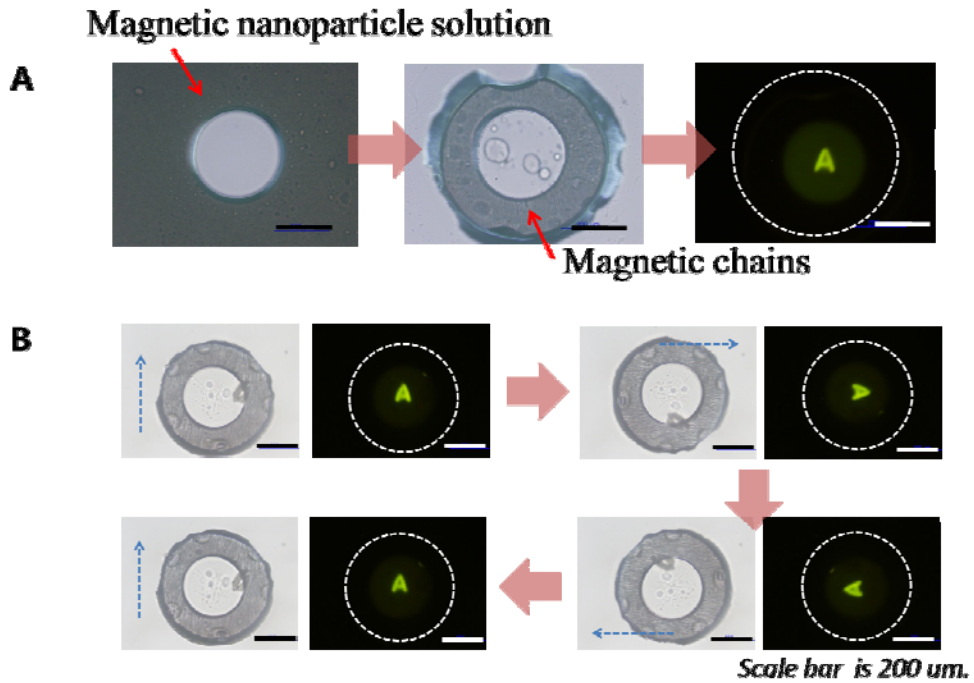


Figure 3.8 Magnetic particle-laden encoded microparticle generation: (A) Fabrication of magnetic-laden particle and its encoding; (B) Rotation of encoded microparticle by the magnetic force. [13]

Recognizing the particle codes when such particles are randomly dispersed in solutions is important. Particles need to be separated from solutions for washing and solution exchange. Thus, magnetic nanoparticles were inserted into the particles, as shown in Figure 3.8. After the magnetic chains were formed by applying a magnetic field to the magnetic nanoparticle solution surrounding the particle, the solution

containing these chains was photopolymerized with UV light to produce double-layered particles. Given that the magnetic chains align along the magnetic field, the double-layered particle can be rotated by changing the direction of the magnetic field. Hence, the codes of particles are easily recognizable regardless of initial orientation. These particles are movable because the magnetic nanoparticles are attracted by magnetic fields. This mobility enables particles to be separated from solutions and facilitates solution exchange and particle washing.

3.2 Multiplexed Assay Platform Using Encoded Microcapsules

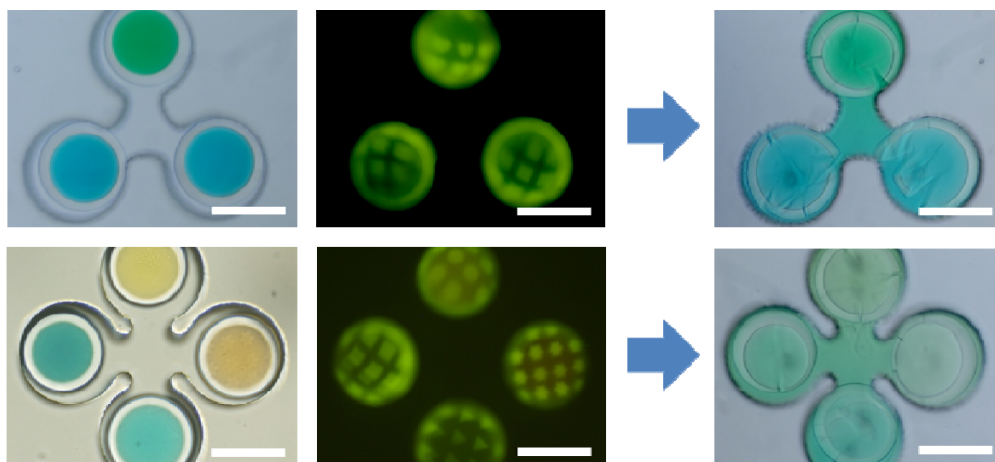


Figure 3.9 Multiplexed assay platform demonstration using encoded microcapsules. The scale bar is 200 μm .

This study demonstrates a new multiplexed assay platform as the first application of

the encoding method using a DMPA photoinitiator. This assay platform uses encoded microcapsules that have liquid cores. To differentiate the liquid types, several food dyes were used to produce PFPE microcapsules. These core-shell microcapsules were encoded using the DMA encoding method. Each microcapsule has a unique code on the shell. These microcapsules were assembled in the PDMS chip. The capsules were broken with a pulsed laser and the liquids from the capsules were released into a common reaction chamber. In the future, real bioassays will be implemented using this new multiplexed assay platform.

3.3 Code-changeable Microparticles for Multi-step Particle-based Assays

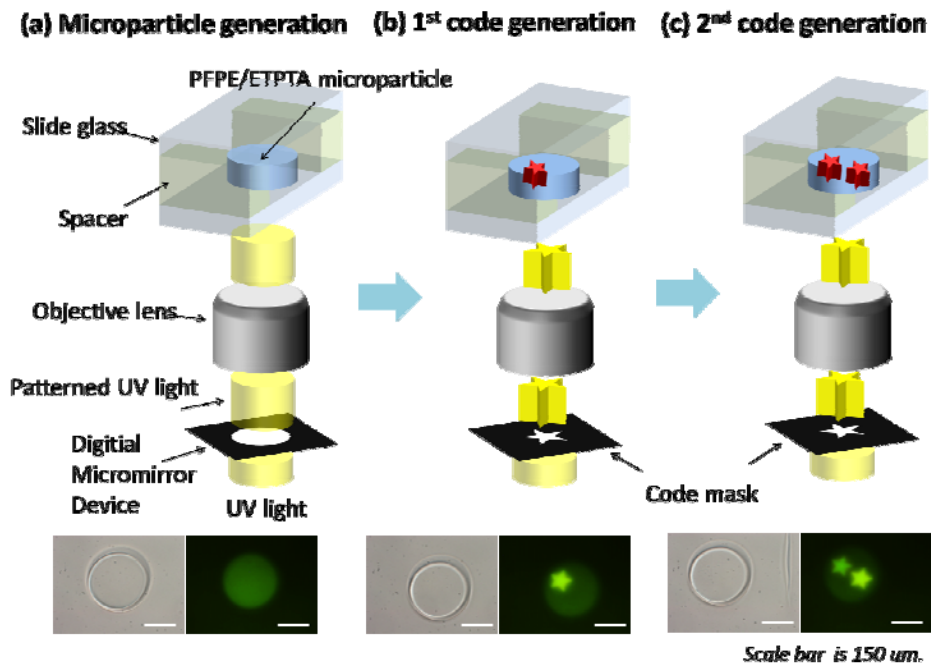


Figure 3.10 Schematic of the generation of code-changeable encoded microparticles using the OFML system. [13]

The new encoding method that uses a photoluminescent material can be applied in “re-writable microparticle” generation. By writing codes repeatedly on the same microparticles, the codes can be continuously changed. The figure above shows the schematic for generating code-changeable microparticles. A mixed solution containing photocurable PFPE and DMPA photoinitiator was introduced between

two glass slides. Patterned UV light from a digital micromirror device was projected onto the mixed solution through an objective lens, after which the PFPE monomers were photopolymerized. UV light with a single-circle pattern was used to generate a disk-shaped microparticle. The bottom figures exhibit the code-changeability of encoded microparticles. A code of this microparticle was created using a star-patterned UV light. By changing the area of UV irradiation, another code was produced on the same particle. These codes emit green light when excited with blue light.

3.3.1 Repeated Code Writing

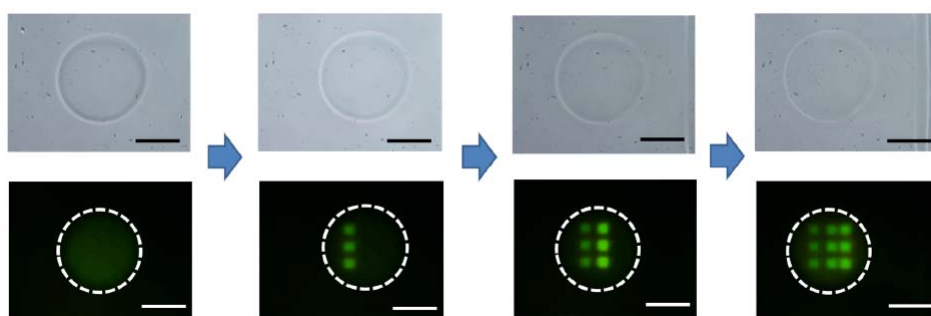
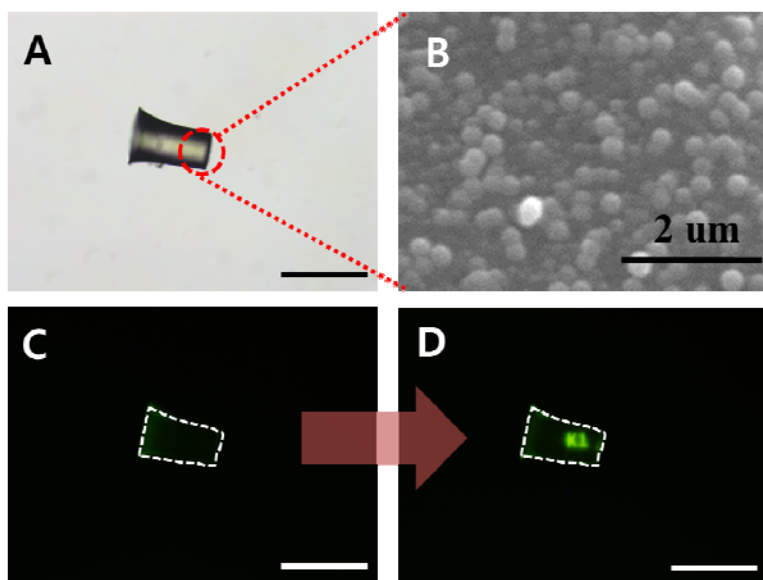


Figure 3.11 Code-changeability of encoded microparticles. The scale bar is 150 μm . [13]

The top figure highlights the code-changeability of the encoding method. In this figure, three squares in a column were sequentially encoded on the same

microparticle. This feature can be used to record the history of biochemical reactions in a microparticle-based assay because codes can be modified after each reaction.

3.3.2 Silica-coating of Code-changeable Microparticles



Scale bar is 200 μm .

Figure 3.12 Silica-coated writable microparticle generation: (A) Bright-field micrograph of silica-coated microparticle; (B) Magnified view of the surface of silica-coated microparticle by scanning electron microscopy; (C) Fluorescent micrograph of the bare silica-coated microparticle; (D) Fluorescent micrograph of the encoded silica-coated microparticle. The scale bar is 200 μm . [13]

To demonstrate that the code-changeable microparticles can be used in a multi-step microparticle-based assay, the particles need to have functional groups. A silica

coating was applied to the particles, as shown in the figures above. The silica coating enables the particles to have functional groups. The modified Stöber method was used to coat the particles with silica [21, 22]. Particles containing the DMPA photoinitiator were silica-coated, and a scanning electron micrograph shows the silica coating around particles. The silica-coated microparticles remained writable. The code “K1” was marked on the silica-coated particle. Aside from generating functional groups, the silica coating prevents the diffusion of the DMPA photoinitiator from the core and it enhances microparticle resistance to strongly acidic and basic environments. In summary, microparticles that contain DMPA photoinitiator were silica-coated to generate functional groups for peptide attachment and for the particle-based assay.

Chapter 4

Conclusion

This thesis presented and characterized a new encoding method for microparticles using the photoluminescent material 2,2-dimethoxy-2-phenylacetophenone (DMPA). This encoding method can be applicable to core-shell microparticle-based multiplexed assays and multi-step microparticle-based assays.

The DMPA photoinitiator is a well-known photocuring agent for acrylic and unsaturated polyester resins, and irradiation under ultraviolet (UV) light triggers photoluminescence. Therefore, photopolymerizable polymers that contain DMPA can have photoluminescent patterns if the additional UV light of patterns is irradiated on them.

To demonstrate feasibility of the encoding method using DMPA photoinitiator, two types of smart particles were fabricated: PFPE core-shell microcapsules and disk-shaped microparticles. First, a polydimethylsiloxane (PDMS) microfluidic channel with a hillock structure was utilized to generate the PFPE core-shell microcapsules, and the partial channel surface was modified to be

hydrophilic using a silane-coupling agent. The flow-focusing configuration produced water–PFPE double emulsions, and the UV irradiation generated core-shell microcapsules. Second, the optofluidic maskless lithography (OFML) system produced disk-shaped PFPE microparticles. The UV light from the digital micromirror device was irradiated to the particle solution through the objective lens. Large-scale particles can be synthesized using an automated microfluidic system.

The OFML setup allowed the easy and fast encoding of microparticles. A patterned UV light was created and projected onto the microparticles. To increase the throughput of the encoding, a simple UV irradiation system with film masks was successfully utilized. Thousands of microparticles can be encoded at once.

The proposed encoding method has several advantages. First, it has code diversity, allowing a variety of graphical codes to be created on the microparticles. Second, the code persists for a long time, remaining identifiable over several weeks so that the encoded microparticles can be used in assays. Third, the code intensity is controllable because the intensity depends on the DMPA concentration and UV irradiation time. In addition, other materials such as magnetic nanoparticles are compatible with the encoding method. Magnetic nanoparticles can be added to the encoded microparticle to facilitate code reading and particle washing.

The proposed encoding method can be applied to multiplexed assay using core-shell microcapsules. Furthermore, multi-step microparticle-based assays, such

as solid-phase peptide synthesis, are possible because the encoded microparticles record sequential biochemical reaction history.

One possible mechanism for such phenomenon is that photolyzed DMPA produces by-products which display photoluminescence. Figure S.1 shows the detailed process of DMPA photolysis [26]. According to this figure, DMPA, a type 1 photoinitiator, generates benzoyl radical and dimethoxybenzyl radical. Dimethoxybenzyl radical produces the colorless liquid methyl benzoate, which, in turn, generates acetophenone, another colorless liquid. In a similar manner, three by-products are produced by benzoyl radicals. When benzoyl radicals acquire hydrogen from the environment, it creates benzaldehyde. When this radical reacts with oxygen, dimethylbiphenyl is produced by sequential reactions. Finally, benzil, a yellowish solid, is generated when benzoyl radicals become dimerized. According to Segurola, methyl benzoate, benzaldehyde, and benzil are the main by-products of DMPA photolysis [26]. When DMPA is photolyzed, its yellow by-products are observed through a bright-field microscope. As UV light intensity increases, the brightness of yellow and the photoluminescence also increase. This phenomenon can likely be explained by the idea that the yellow by-products of DMPA photolysis can contribute to photoluminescence. As discussed earlier, DMPA produces several yellow by-products, such as benzil, when irradiated by UV light. Therefore, benzil can be considered as a candidate material for producing DMPA photoluminescence.

Another possible mechanism for DMPA photoluminescence is that the surrounding medium, such as liquid or solid, as well as the by-products of photolysis

of the DMPA photoinitiator, can affect photoluminescence. Photoluminescence intensity depends on the solution environment. The solvent can affect the process of electron transition in which electrons absorb high energy from UV or visible light, acquire excited states, and emit light with longer wavelengths. When a photoluminescent material is in a solid, its photoluminescence intensity can be increased. Before UV irradiation, double emulsions are not yet photopolymerized. The outer shells of these double emulsions consist of uncured monomers and DMPA photoinitiators. Under this state, double emulsions have low photoluminescence. After double emulsions are irradiated with UV, the DMPA photoinitiator is photolyzed and uncured monomers are cross-linked. Monomers are not yet fully photopolymerized; therefore, liquids and solids coexist. Compared with the previous state, this state results in the DMPA photoinitiator being surrounded by a solid environment. Consequently, increased photoluminescence is observed on the shells of the microcapsules. A patterned UV light is applied to the shells to generate codes on them. Additional UV irradiation allows denser cross-linking of monomers and finally creates a solid state. The DMPA photoinitiator exhibits increased photoluminescence because it is surrounded only by a solid. This increased photoluminescence of patterns creates codes for the microcapsules.

Bibliography

- [1] S. Birtwell and H. Morgan, “Microparticle encoding technologies for high-throughput multiplexed suspension assays,” *Integrative Biology*, vol. 1, pp. 345–362, 2009. [국제저널지]
- [2] S. E. Chung, W. Park, H. Park, et al., “Optofluidic Maskless Lithography System for real-time synthesis of photopolymerized microstructures in microfluidic channels,” *Applied Physics Letters*, vol. 91, no. 4, pp. 041106, 2007. [국제저널지]
- [3] Y. Zhao, X. Zhao, B. Tang, et al., “Quantum-Dot-Tagged Bioresponsive Hydrogel Suspension Array for Multiplex Label-Free DNA Detection,” *Advanced Functional Materials*, vol. 20, no. 6., pp. 976–982, 2010. [국제저널지]
- [4] Y. Li, Y. T. Hong, and D. Luo, “Multiplexed detection of pathogen DNA with DNA-based fluorescence nanobarcodes,” *Nature Biotechnology*, vol. 23, pp. 885–889, 2005. [국제저널지]

- [5] L. Grondahl, B. J. Battersby, D. Bryant, et al., “Encoding combinatorial libraries: A novel application of fluorescent silica colloids,” *Langmuir*, vol. 16, pp. 9709–9715, 2000. [국제저널지]
- [6] B. J. Battersby, D. Bryant, W. Meutermans, et al., “Toward larger chemical libraries: Encoding with fluorescent colloids in combinatorial chemistry,” *Journal of the American Chemical Society*, vol. 122, pp. 2138–2139, 2000. [국제저널지]
- [7] B. J. Battersby, G. A. Lawrie, and M. Trau, “Optical encoding of microbeads for gene screening: alternatives to microarrays,” *Drug Discovery Today*, vol. 6, pp. 19–26, 2001. [국제저널지]
- [8] M. Trau and B. J. Battersby, “Novel colloidal materials for high-throughput screening applications in drug discovery and genomics,” *Advanced Materials*, vol. 13, pp. 975–979, 2001. [국제저널지]
- [9] A. M. Ganan-Calvo, L. Martin-Banderas, R. Gonzalez-Prieto, et al., “Straightforward production of encoded microbeads by Flow Focusing: Potential applications for biomolecule detection,” *International Journal of Pharmaceutics*, vol. 324, pp. 19–26, 2006. [국제저널지]

- [10] D. K. Wood, G. B. Braun, J. -L. Fraikin, et al., “A feasible approach to all-electronic digital labeling and readout for cell identification,” *Lab on a Chip*, vol. 7, pp. 469-474, 2007. [국제저널지]
- [11] D. C. Pregibon, M. Toner, and P. S. Doyle, “Multifunctional Encoded Particles for High-Throughput Biomolecule Analysis,” *Science*, vol. 315, pp. 1393-1396, 2007. [국제저널지]
- [12] S. Han, H. J. Bae, J. Kim, S. Shin, S.-E. Choi, S. H. Lee, S. Kwon, W. Park, “Lithographically Encoded Polymer Microtaggant Using High-Capacity and Error-Correctable QR Code for Anti-Counterfeiting of Drugs,” *Advanced Materials*, vol. 24, pp. 5924-5929, 2012. [국제저널지]
- [13] T. Kwon, Y. Song, D. Lee, et al., “Code-changeable Encoded Microparticles for Multi-step Bead-based Assay,” *The 17th International Conference on Miniaturized Systems for Chemistry and Life Sciences (MicroTAS) 2012*, (Accepted). 2012. [국제학술대회]
- [14] Y. Song, T. Kwon, D. Lee, et al., “Liquid Capped Encoded Microshell and Partipetting for Ultraplexed Liquid Assay,” *The 25th Institute of Electrical and Electronics Engineers (IEEE)*

International Conference on MEMS 2012, 965-968, 2012.

[국제 학술대회]

[15] C. Kim, S. Chung, Y. E. Kim, et al., "Generation of core-shell microcapsules with three-dimensional focusing device for efficient formation of cell spheroid," *Lab on a Chip*, vol. 11, pp. 246-252, 2011. [국제저널지]

[16] M. Zagnoni, J. Anderson, and J. M. Cooper, "Hysteresis in Multiphase Microfluidics at a T-junction," *Langmuir*, vol. 26, pp. 9416-9422, 2010. [국제저널지]

[17] M. A. Fowzy, "PFPE, A Unique Lubricant for a Unique Application," Castrol Industrial North America, Specialty products division, developed data at the R&D lab in downers grove, Illinois 1998. [기술자료]

[18] HUSK-ITT Corp., "Applications and Benefits of Perfluoropolyether (PFPE) Lubricants," HUSKEY Specialty Lubricants, 2005. [기술자료]

[19] R. Bongiovanni, A. Medici, A. Zompatori, et al., "Perfluoropolyether polymers by UV curing: design, synthesis and characterization," *Polymer International*, vol. 61, pp. 65-73, 2012. [국제저널지]

- [20] A. Vitale, M. Quaglio, M. Cocuzza, et al., "Photopolymerization of a perfluoropolyether oligomer and photolithographic processes for the fabrication of microfluidic devices," *European Polymer Journal*, vol. 48, pp. 1118-1126, 2012. [국제저널지]
- [21] W. Stöber, A. Fink, and E. Bohn, "Controlled growth of monodisperse silica spheres in the micron size range," *Journal of Colloid and Interface Science*, vol. 26, pp. 62-69, 1968. [국제저널지]
- [22] J. Ge and Y. Yin, "Magnetically Tunable Colloidal Photonic Structures in Alkanol Solutions," *Advanced Materials*, vol. 20, pp. 3485-3491, 2008. [국제저널지]
- [23] J. -P. Fouassier and A. Merlin, "Laser Investigation of Norrish Type I Photocission in the Photoinitiator Irgacure (2,2-dimethoxy 2-phenyl-acetophenone)," *Journal of Photochemistry*, vol. 12, pp. 17-23, 1980. [국제저널지]
- [24] J. E. Baxter, R. S. Davidson, H. J. Hageman, et al., "A study of the photodecomposition products of an acylphosphine oxide and 2,2-dimethoxy-2-phenylacetophenone," *Polymer*, vol. 29, pp. 1575-1580, 1988. [국제저널지]

- [25] H. Fischer, R. Baer, R. Hany, et al., "2,2-Dimethoxy-2-phenylacetophenone: Photochemistry and Free Radical Photofragmentation," *Journal of the Chemical Society, Perkin Transactions 2*, pp. 787-798, 1990. [국제저널지]
- [26] J. Segurola, N. S. Allen, M. Edge, et al., "Photoyellowing and discolouration of UV cured acrylated clear coatings systems: influence of photoinitiator type," *Polymer Degradation and Stability*, vol. 64, pp. 39-48, 1999. [국제저널지]
- [27] V. Mucci and C. Vallo, "Efficiency of 2,2-Dimethoxy-2-phenylacetophenone for the Photopolymerization of Methacrylate Monomers in Thick Sections," *Journal of Applied Polymer Science*, vol. 123, pp. 418-425, 2011. [국제저널지]

발광 물질을 이용한 새로운 마이크로입자 코드화 기법 및 응용

바이오 의학 연구 분야에서 다중 분석 기술은 유전자 형질을 분석하고, 효과가 있는 약물을 검색하거나 병을 진단할 때 유용하게 사용되어왔다. 처리량이 많고, 사용자가 편리하게 사용할 수 있으며, 가격이 싼 다중 분석 방법들 중 하나로써, 코드화된 입자 방법이 있다. 코드화된 입자를 이용하면 다양한 분자들을 쉽게 다룰 수 있다. 분자들이 있는 액체 자체를 미세입자로 운반하고, 각 분자들을 확인하기 위해서는 새로운 마이크로입자가 필요하며, 이와 동시에 해당 입자를 코드화할 수 있는 기법이 개발되어야 한다. 본 논문에서는 2,2-dimethoxy-2-phenylacetophenone (DMPA) 광개시제의 발광 현상을 이용하여 미세입자에 적합한 새로운 코드화 방식을 소개하고, 이 방식이 다중 분석 기술에 응용될 수 있음을 보인다. 먼저, Perfluoropolyether 로 된 마이크로캡슐과 디스크 형태의 마이크로입자를 미세유체학과 광미세유체 마스크리스 리소그래피를 이용하여 제작하였다. 다양한 패턴의 자외선을 조사하여 이 입자들에 코드를 생성하였다. 이러한 입자 코드화 방식은 다양한 패턴을 생성할 수 있어 많은 수의 코드를 생성할 수 있고, 오랜 시간 동안 코드가 유지되는 장점을 가진다. 코드의 세기는 DMPA 의 농도와 UV 조사량에 의해 조절될 수 있다. 이 입자 코드화 방식은

실제 다중 분석 기술에 유용하게 쓰일 수 있고, 다단계 생화학 반응을 추적하는 데에도 사용될 수 있다.

주요어 : 다중 분석 기술, 마이크로입자, 코드화, 발광, 미세유체학

학번 : 2011-20794